Crowding Effects on the Formation and Maintenance of Nuclear Bodies: Insights from Molecular-Dynamics Simulations of Simple Spherical Model Particles

Eun Jin Cho[†] and Jun Soo Kim[‡*]

[†]Department of Chemistry and Applied Chemistry, Hanyang University, Kyeonggi-do, Republic of Korea; and [‡]Department of Chemistry and Nano Science, Ewha Womans University, Seoul, Republic of Korea

ABSTRACT The physics of structure formation and maintenance of nuclear bodies (NBs), such as nucleoli, Cajal bodies, promyelocytic leukemia bodies, and speckles, in a crowded nuclear environment remains largely unknown. We investigate the role of macromolecular crowding in the formation and maintenance of NBs using computer simulations of a simple spherical model, called Lennard-Jones (LJ) particles. LJ particles form a one-phase, dilute fluid when the intermolecular interaction is weaker than a critical value, above which they phase separate and form a condensed domain. We find that when volume-exclusive crowders exist in significant concentrations, domain formation is induced even for weaker intermolecular interactions, and the effect is more pronounced with increasing crowder concentration. Simulation results show that a previous experimental finding that promyelocytic leukemia bodies disappear in the less-crowded condition and reassemble in the normal crowded condition can be interpreted as a consequence of the increased intermolecular interactions between NB proteins due to crowding. Based on further analysis of the simulation results, we discuss the acceleration of macromolecular associations that occur within NBs, and the delay of diffusive transport of macromolecules within and out of NBs when the crowder concentration increases. This study suggests that in a polydisperse nuclear environment that is enriched with a variety of macromolecules, macromolecular crowding not only plays an important role in the formation and maintenance of NBs, but also may perform some regulatory functions in response to alterations in the crowding conditions.

INTRODUCTION

A cell nucleus is highly compartmentalized and contains numerous nuclear bodies (NBs), such as nucleoli, Cajal bodies, promyelocytic leukemia (PML) bodies, and speckles. NBs are morphologically distinct, with roughly spherical shapes ranging in size from several hundred nanometers to several micrometers, and are not surrounded by physical boundaries (e.g., membranes), which allows the dynamic exchange of constituting macromolecules (i.e., body-specific proteins and RNAs). Based on the role of their constituting proteins in these biological processes, and the association of NBs with specific gene loci, it has been suggested that NBs play functional roles in transcription and RNA processing (1–6); however, the physics of their structure formation and maintenance have not been well understood. For instance, it was not known whether structural assembly occurs in a specific order or in a random fashion, and only recently has some important evidence been obtained in support of the idea that NBs are formed by a random assembly of constituting proteins (7). More recently, it was also shown that body-specific RNAs can nucleate the formation of NBs (6,8).

NBs are formed in intrinsically crowded environments. A cell nucleus is a very crowded space with a high content of macromolecules, and the total nuclear volume occupied by these macromolecules, including chromosomes, is in the range of $\geq 20\%$. In general, macromolecules that are not involved in a specific biological process under investigation are referred to as crowders. Among various nuclear macromolecules, many proteins are not associated with any nuclear structure and instead are found diffusely throughout nucleoplasm (9), and therefore are referred to as crowders in this work. Although some other nuclear proteins have been reported to be associated with some specific nuclear structures, they may also be considered as crowders when they are not associated with a specific type of NB under investigation.

Previous experimental and theoretical studies with model crowders indicated that macromolecular crowding is important in the structure formation of biomolecules and in the reaction equilibrium and kinetics of macromolecular associations (10–14). Recently, it was suggested that crowding plays a role in the compaction of chromatin fibers and formation of other nuclear structures (15–19). The effect of crowding is usually explained by the entropically driven depletion attraction induced between a pair of macromolecules by the presence of other macromolecules, which becomes more significant as the crowding concentration increases (18,20,21). Because NB proteins are known to self-interact to form NBs (2,4,22), and they exist in crowded nuclear environments, it seems obvious that macromolecular crowding should play an important role in the formation and maintenance of such NBs. In fact, a recent experimental study showed that nucleoli and PML bodies are dissembled under less crowded conditions and reassemble when crowders are added (15).

Submitted June 6, 2012, and accepted for publication July 5, 2012.

*Correspondence: jkim@ewha.ac.kr

Editor: Michael Edidin.

0006-3495/12/08/0424/10 $2.00

http://dx.doi.org/10.1016/j.bpj.2012.07.007

In this study, we investigate the role of macromolecular crowding in the structure formation and maintenance of NBs using computer simulations of a simple spherical model, known as Lennard-Jones (LJ) particles. We first focus on the marked effect of macromolecular crowding on the self-assembly of LJ particles mimicking the structure formation of NBs by comparing phase separation in the absence and presence of crowders. We then address the more interesting issue of the physical consequences that might arise when the crowding condition changes. Situations in which the crowding condition changes are discussed briefly in the Results and Discussion section. A change in the crowding condition will definitely result in structural alterations of NBs, possibly leading to a change in their biological functions. However, due to the divergent roles of crowding in the stability of macromolecular complexes and the dynamics of the constituting macromolecules, it is not easy to predict whether a change in the crowding condition will induce favorable consequences for specific biological functions. Therefore, we limit our discussion to a few physical consequences that might affect these biological functions (i.e., the diffusive transport of macromolecules and their associations within NBs) when the crowding condition changes.

The simple spherical LJ particles employed in this work have a spherical shape and interact with each other through an LJ potential with volume-exclusive repulsions at short distances and moderate attractions beyond. Clearly, LJ particles are too simple to model various NB proteins having different shapes, interactions, and compositions. However, our choice of the simple spherical particles is based on the lack of structural information about key proteins and the impracticability of computer simulations with all details at the atomistic level. For example, we lack structural information about important NB proteins such as survival motor neurons and coilin, which are the key components of the Cajal bodies. Even with such information, computer simulations of these proteins in a solution are not practically achievable with details at the atomistic level. NBs are composed of various components whose copy number exceeds several tens or hundreds. Simulations of even a single protein with atomistic details can be performed only up to a few microseconds (the maximum of a millisecond was recently obtained with a highly specialized computer (23)). To study the assembly of NBs in the crowded nucleus, it may be necessary to perform simulations of several tens of thousands of proteins on a timescale longer than minutes, and such computations are not currently possible with the modern computers typically at hand.

The most basic feature of NB proteins is their self-interaction to form the assembled structure. Recently, it was reported that any Cajal body protein can nucleate the formation of the entire CB structure de novo (7). Among all possible models that self-interact, LJ particles are one of the simplest models whose phase separation has other physical similarities with NB formation. LJ particles can phase-separate into condensed and dilute phases, and these phases are not separated by any physical boundary. Thus, LJ particles can be dynamically exchanged between the condensed and dilute phases. These are the common features seen in NB formation. Therefore, we believe that, although they are not perfect for describing the detailed mechanisms of NB formation, LJ particles can provide important insights into the formation and maintenance of NBs, especially in a crowded environment. In the remainder of this work, we refer to LJ particles as NB particles because they mimic the self-interaction of the proteins and RNAs of NBs.

To understand the effect of macromolecular crowding on the domain formation of NB particles (i.e., NB formation), we perform molecular-dynamics (MD) simulations of a preformed condensed domain of NB particles at various interaction strengths, and compare the stability of the domain in the absence and presence of crowders. When the domain remains stable after MD simulations, the condensed phase is in equilibrium with the dilute phase, and we conclude that phase separation can occur at the given interaction strength between NB particles. Recently, we published a related work using similar simulations for systems with an elongated cuboidal geometry (24). For strong attractions between NB particles, the condensed domain in the middle of the simulation system along the elongated axis is in equilibrium with the dilute phase, and the use of periodic box images actually describes the formation of an infinitely connected and thin layer. However, the shape of NBs is roughly spherical. Therefore, we extend our previous research to the formation of spherical domains composed of NB particles. Unlike the previous work, in which we did not discuss any further consequences of crowding other than formation of the condensed phase, here we also discuss the effect of crowding on the physical properties of the condensed domain. More specifically, we discuss the biological implications of crowding in terms of molecular associations that occur within NBs, such as the assembly of U4/U6 spliceosomal di-snRNPs (25), and their transport within and out of the domain. In addition, we perform additional constraint-biased MD simulations to calculate the effective depletion potential between NB particles induced by crowders, which is used as a direct explanation of crowding-promoted domain formation.

In this work, we focus mostly on the effects induced by the presence of volume-exclusive, repulsive crowders. Proteins do not deeply penetrate each other, and such an effect is qualitatively described by repulsive interactions between crowders and NB particles, and between the crowders themselves. In addition, proteins may have weak attractive interactions, such as van der Waals interactions, and weak electrostatic interactions with other proteins. Because we lack quantitative data for protein-protein and

protein-RNA interactions, it is difficult to evaluate the attraction strength that is applicable to our model of crowders. However, based on the previous experimental observation by Hancock (15) that crowding promotes the formation of NBs, we assume that the attraction between crowders and NB proteins cannot be so strong as to disassemble NBs. In our previous work, we studied the effect of crowders having attractive interactions with NB particles, as well as with themselves, by varying the attraction of the crowders in a range between weak and moderate strengths (24). Although the presence of attractive crowders reduces the phase separation induced by repulsive crowders, the excluded-volume effect of repulsive crowders is still significant in the presence of attractive crowders unless their attraction strength is too large (24). Therefore, we limit our discussion in this work to crowding effects induced by repulsive crowders, to mimic the presence of proteins that are found diffusely throughout the nucleoplasm and are not associated with any specific nuclear structure (9).

MATERIALS AND METHODS

MD simulations for phase separation of NB particles

We perform classical MD simulations of systems containing NB particles in the absence and presence of crowders. The first set of simulations is performed for single-component NB particles in varying intermolecular interactions to determine their phase diagram in the absence of crowders. The phase diagram depicts the range of intermolecular interactions between NB particles in which their phase separation occurs, and the densities of the condensed and dilute phases when it occurs. In the second set of simulations, we examine systems containing not only NB particles but also cosolute macromolecular crowders to understand how the presence of macromolecular crowders changes the range of NB interactions for phase separation. By assessing whether the phase separation occurs at the same density in both sets of simulations, and comparing the interactions of NB particles in the simulations, we can understand the effect of macromolecular crowding on the phase separation of NB particles.

Both sets of simulations start with a preformed, large condensed domain of NB particles at varying intermolecular interactions between NB particles. By inspecting the simulation trajectories and calculating the density profile of the NB particles, we find the range of NB interactions for which the domain remains stable for crowder volume fractions of 0.00, 0.05, 0.10, and 0.15. At each value of NB interactions within such range, the condensed domain reaches equilibrium with the dilute phase in the initial course of MD simulations. For the same interaction strength, a system will always attain such phase separation independently of the initial distribution of NB particles, resulting in the same average density and size of a condensed domain. If the initial condensed domain is denser or larger than the equilibrium condensed domain at the given interaction strength, the equilibrium will be attained by losing some NB particles in the dilute phase. On the other hand, when simulations are run for systems with randomly distributed NB particles at the same interaction strength, phase separation into the condensed and dilute phases will occur by the nucleation of small condensed domains, followed by their aggregation into a single, large condensed domain, which is true in this work because the total density of NB particles is low (26). To verify this statement, we performed three additional simulations starting with randomly distributed NB particles at the crowder volume fraction of 0.10 and at three different interaction strengths within a range for phase separation. The formation of a single large domain was verified: the domain formation is initiated by a nucleation process that results in several small condensed domains, and eventually a single large domain is formed by their diffusion and aggregation (26).

Therefore, although the results presented in this work were all obtained from simulations starting with a preformed, large condensed domain, the results are interpreted in terms of the phase separation and the formation of a condensed domain. Hereafter, we interpret the range of NB particle interactions for which a preformed condensed domain remains stable as the range of the interactions for which the phase separation occurs and a condensed domain is formed.

NB particles interact with each other via the LJ potential $U(r) = 4\epsilon_{NB}[(\sigma/r)^{12} - (\sigma/r)^{6}]$, where ϵ_{NB} is the attraction strength between NB particles and σ corresponds to the particle diameter. The potential is truncated and shifted at the cutoff radius of 2.5σ. Crowders interact via purely repulsive potentials with NB particles as well as with themselves. The interaction potential for crowders has the same functional form but with a different cutoff radius of $2^{1/6}\sigma$, so that the potential of crowders contains only the purely repulsive part of the LJ potential. The interaction strength ε of crowders is set at 1.0 and their diameter is set at 1σ.

All simulations are performed at constant N, V, and T, with GROMACS version 4.5.4 (27). To investigate the crowding effect systematically at each fixed value of the crowder volume fraction, we run the simulations at constant volume instead of at constant pressure (24). The simulation system has a cubical dimension of $60\sigma \times 60\sigma \times 60\sigma$, containing 20,625 NB particles and 20,625, 41,250, and 61,850 crowders for crowder volume fractions, ϕ, of 0.05, 0.10, and 0.15, respectively. The number of NB particles (corresponding to a reduced density of $\rho_{NB}\sigma^3 = 0.0955$) is chosen such that the condensed domain with a spherical shape (when the phase separation occurs) is formed in equilibrium with the dilute phase. The crowder volume fractions of 0.05, 0.10, and 0.15 are chosen to mimic the protein density in the nucleoplasm of *Xenopus* oocyte with 0.106 g/cm^3 (the volume fraction is calculated as 0.077 using a specific volume of 0.73 cm^3/g) (28). Higher volume fractions of crowders may be more relevant when the volume occupation by chromosomes is also taken into account. Although the crowding effect may be more enhanced at higher crowder volume fractions, the qualitative conclusions will not change significantly.

Initial configurations for all sets of simulation are prepared such that NB particles are condensed in the middle of the simulation system, forming a spherical interface between the condensed and dilute phases. When crowders are included, crowders are distributed in the rest of the simulation volume. MD simulations are performed at a reduced temperature ($T^* = k_B T/\epsilon_{NB}$) ranging between 0.65 and 1.50 depending on the crowding volume fraction, where k_B is the Boltzmann constant and T is the temperature. Equations of motion are integrated using the leapfrog algorithm with a time step (δt) of $0.01\tau_{MD}$, where $\tau_{MD} = \sigma(m/\epsilon_{NB})^{1/2}$. A total of 1.2×10^7 time steps ($1.2 \times 10^5 \tau_{MD}$) is run for each simulation and the trajectories are stored every 10^3 time steps. The trajectories of 1×10^7 time steps after the equilibration in the first 2×10^6 time steps are used to calculate the equilibrium densities of the condensed and dilute phases.

For systems with a stable condensed domain, we calculate the densities of the condensed and dilute phases by the method described below. The direct calculation of densities in the condensed and dilute phases from simulations is complicated due to the existence of identical NB particles in both phases. It is difficult to distinguish NB particles in the condensed phase from those in the dilute phase unless some criteria are given for a clear distinction between NB particles in the two phases. Although it is not impossible to find such criteria, for instance, by counting the number of nearest neighbor particles in each phase, the distinction is not very clear near an interfacial region. Instead, we calculate the densities in the two phases by determining the radial density profiles and fitting them into Eq. 1, the use of which has been well established for studying the vapor-liquid phase separation of single-component LJ particles (29,30). For all sets of simulations, the average density profiles of NB particles at each $k_B T/\epsilon_{NB}$ are calculated in the radial direction from the center of mass of a condensed domain, after the center of mass of the condensed domain is

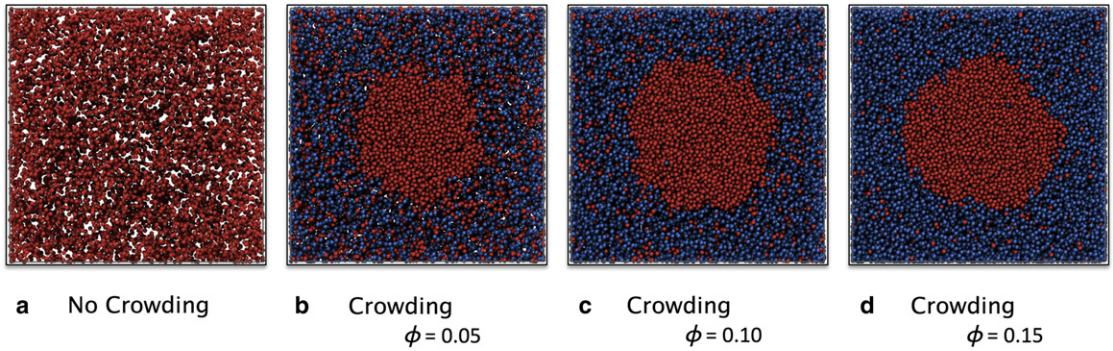

FIGURE 1 Cross-sectional view of simulation systems at $k_BT/\epsilon_{NB} = 1.00$. Whereas NB particles form a one-phase fluid in the absence of crowders, as shown in *a*, the domain formation of NB particles is observed in the presence of crowders, as in *b–d*, and becomes more pronounced as ϕ increases.

translated to the center of simulation system at each time step. The densities of the condensed and dilute phases are determined by fitting the density profile to the following equation:

$$\rho(r) = \frac{1}{2}(\rho_{dense} + \rho_{dilute}) - \frac{1}{2}(\rho_{dense} - \rho_{dilute}) \tanh\frac{2(r-w)}{d}, \quad (1)$$

where r is the distance from the center of mass of the condensed phase, w is the effective radius of the condensed phase, d is the interfacial thickness, and ρ_{dense} and ρ_{dilute} are the densities of the condensed and dilute phases, respectively. The validity of this method has been confirmed by comparison with results from other computational methods, such as the Gibbs ensemble method and the grand ensemble method (29). The determination of the densities from the nonlinear fitting into Eq. 1 is also advantageous because it also provides the values of w and d. We verify that the nonlinear fit overlaps very well with the simulation density profile for each simulation set.

In addition, we also perform constraint-biased MD simulations to calculate the potential of mean force. The potential of mean force is the interaction between two NB particles at a given distance, averaged over all the degrees of freedom of the molecules in the environment. The change in the crowding condition influences the interaction between two NB particles, and therefore it provides a direct assessment of the crowding effect on the intermolecular association between NB particles. Details on the method used to calculate the potential of mean force are included in the Supporting Material.

Calculation of the physical properties of a condensed domain

The physical consequences of the altered crowding condition are investigated in terms of the diffusive transport of NB particles within NBs and out to the nucleoplasmic space, and the rate of macromolecular associations occurring within NBs. First, we investigate the crowding effect on the diffusive transport of NB particles by calculating the first passage times for central NB particles to reach specific radial distances in and out of the condensed domain. The central NB particles are defined as those located within a distance of 3.0 σ from the center of mass of the condensed domain. The first passage time to specific distances in and out of the domain provides information about the diffusive transport of macromolecules within NBs and out to the nucleoplasmic space. Second, when the density of the condensed domain changes in different crowding conditions, the macromolecular association within the condensed domain is also subject to change. The rate of macromolecular associations is calculated using theoretical predictions developed for the diffusion-controlled reaction, called the Smoluchowski theory. Previously, the validity of the theoretical prediction for the rate constant in a crowded environment was verified by comparison with Brownian dynamics simulations, and therefore we adopt the same method with modified parameters suitable for this work (13,14,31). Details regarding these calculations are also described in the Supporting Material.

RESULTS AND DISCUSSION

Fig. 1 shows cross sections of four simulated systems at $k_BT/\epsilon_{NB} = 1.00$ in the absence of crowders (Fig. 1 *a*), and in the presence of crowders with volume fractions of 0.05, 0.10, and 0.15 (Fig. 1, *b–d*, respectively). At $k_BT/\epsilon_{NB} = 1.00$, NB particles in the absence of crowders form only a one-phase fluid without phase separation. When crowders are added to the system, the NB particles phase separate. As the crowding volume fraction ϕ increases, the phase separation becomes even clearer. Because the formation of a condensed domain by phase separation of NB particles mimics the formation of an NB, the terms are used interchangeably in this context.

Phase separation and domain formation of NB particles in the absence of crowders

Average radial density profiles and a phase diagram are presented in Fig. 2, *a* and *b*. At each time in the simulation trajectories, the center of mass of a condensed phase is first determined and the density of NB particles is calculated radially from its center of mass. The radial density profiles in Fig. 2 *a* calculated at $k_BT/\epsilon_{NB}<1.00$ show a clear distinction between condensed and dilute phases. The interface between the two phases becomes broader as k_BT/ϵ_{NB} increases up to 0.95. We calculate the average densities of NB particles in condensed and dilute phases by fitting the density profiles to Eq. 1. As k_BT/ϵ_{NB} increases (i.e., as the attraction between NB particles decreases), the density of the condensed phase decreases and that of the dilute phase increases until the NB particles form only one fluid phase without phase separation, which corresponds to $k_BT/\epsilon_{NB} \geq 1.00$.

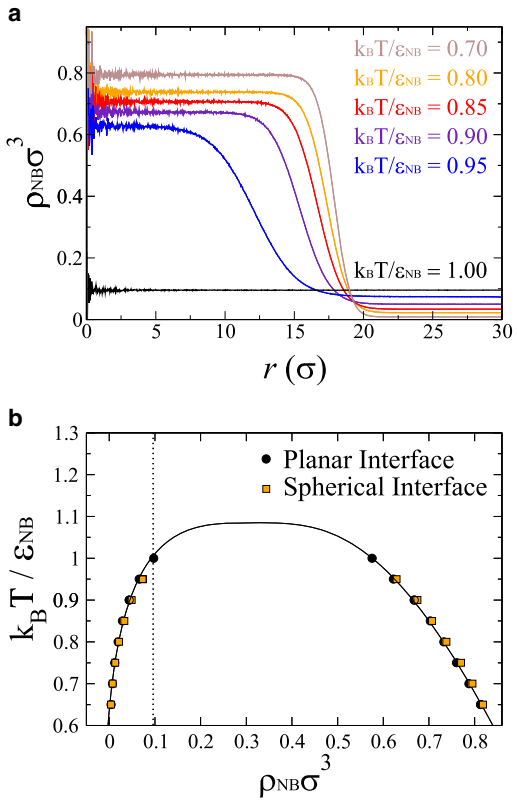

FIGURE 2 Phase separation of NB particles in the absence of cosolute crowders. (*a*) Radial density profiles of NB particles for different k_BT/ϵ_{NB} -values ranging between 0.70 and 1.00 from top to bottom. (*b*) Phase diagram of NB particles depicting a range of the reduced temperature k_BT/ϵ_{NB} and the reduced density $\rho_{NB}\sigma^3$. Square symbols indicate the densities obtained in this work with a spherical interface, and circles indicate data obtained in our previous work with a planar interface (24). The solid line in *b* is a curve fitted to circles, and the dotted line at $\rho_{NB}\sigma^3 = 0.095$ is to mark the density of NB particles.

Measured densities $\rho_{NB}\sigma^3$ for the dense and dilute phases at each k_BT/ϵ_{NB} are depicted in the phase diagram shown in Fig. 2 *b*. For any system with ($\rho_{NB}\sigma^3$,k_BT/ϵ_{NB}) located in a region under the phase boundary, phase separation into dense and dilute phases will be observed. As shown in Fig. 2 *b*, the phase diagram determined in this work is almost identical to that obtained in our previous work (24), which was calculated for phase-separated NB particles forming a planar interface between two phases. One of the main differences between these two studies is that in the work presented here, there was a smaller density of NB particles in the entire simulation system (0.095 in this work compared with 0.24 in the previous work). The change of k_BT/ϵ_{NB} from top to bottom along the dotted line (marking the density of 0.095) in Fig. 2 *b* results in the transition from a one-phase fluid to a fluid with two phases when k_BT/ϵ_{NB} is reduced to <1.00. Therefore, the range of k_BT/ϵ_{NB} in which the phase separation of NB particles is observed is reduced (k_BT/ϵ_{NB} <1.00 in this work and k_BT/ϵ_{NB} <1.10 in the previous work).

Crowding-induced domain formation of NB particles

Fig. 1 shows that the phase separation of NB particles is facilitated by the presence of crowders: at $k_BT/\epsilon_{NB} = 1.00$, NB particles do not phase separate in the absence of crowders, whereas phase separation occurs in their presence. The facilitated phase separation by crowders is depicted more clearly in Fig. 3, where the sets of simulation point (ϕ,k_BT/ϵ_{NB}) are marked as squares (with phase separation) or triangles (without phase separation) depending on the occurrence of phase separation. In the absence of crowders ($\phi = 0$), the phase separation of NB particles is observed when k_BT/ϵ_{NB} <1.00, whereas a one-phase fluid is observed at larger k_BT/ϵ_{NB}. However, in the presence of crowders, the phase separation of NB particles is observed even at $k_BT/\epsilon_{NB} > 1.00$. This implies that the crowders can promote the phase separation of NB particles even under the condition where it never occurs in the absence of crowders, as shown in Fig. 1. The increase of the range of k_BT/ϵ_{NB} in which phase separation is observed (marked with *square symbols* in Fig. 3) indicates that phase separation can occur for weaker attractions between NB particles. This crowding-facilitated phase separation becomes more significant as ϕ increases.

Experimental data on the role of crowding in the maintenance of NBs (15) can be interpreted on the basis of the results in Fig. 3. When cells were incubated in the media with low salt concentration, they became swollen and the nucleus became less crowded. In such cases, the NBs disappeared and nucleolar transcript elongation fell by ~85%. However, when the cells were reincubated in the normal nuclear buffer, NBs were formed again. Of interest, NBs also re-formed when inert crowders such as dextran and polyethylene glycol were added to the swollen nucleus and the nuclear environment again became crowded. Therefore, it can be conjectured that, in the absence of crowders, the attraction strength of NB proteins and RNAs may not be

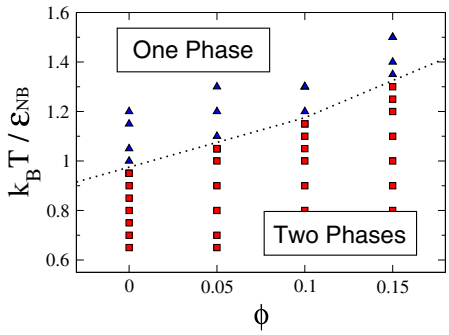

FIGURE 3 Range of k_BT/ϵ_{NB} for phase separation at different ϕ-values. Square symbols represent values of k_BT/ϵ_{NB} at which phase separation occurs, and triangles indicate those at which a one-phase fluid is observed. The dotted line separates the one- and two-phase regions and is included to guide the eye.

large enough to form NBs, that is, k_BT/ϵ_{NB} may be ≥ 1.00, so that the phase separation does not occur without crowders. When crowders are added and the nucleus becomes crowded ($\phi > 0$), the phase separation is observed for the same k_BT/ϵ_{NB}, explaining the role of inert crowders in the reassembly of NBs in the experiment (15).

When the radial density profiles are fitted to Eq. 1, not only densities but also a radius of the domain and the interfacial thickness between two phases are obtained. The changes in the density and size of the domain are depicted in Fig. 4. Of interest, both the size of the domain and its density increase with crowding, which implies that more NB particles participate in the formation of the condensed domain. Therefore, we can conclude that the macromolecular crowding does not just confine NB particles into a smaller volume, thereby increasing the density, but must also induce the effective attraction between NB particles so that more NB particles can assemble.

Direct evidence of the increase of the effective attraction due to crowding is provided by the potential of mean force shown in Fig. 5. The potential of mean force is obtained from the constraint-biased MD simulations in the crowded system, as described in the Supporting Material. In Fig. 5, the attractive well depth becomes greater by ~0.1 or 0.2 k_BT each as ϕ increases from 0.00 to 0.15. The change of

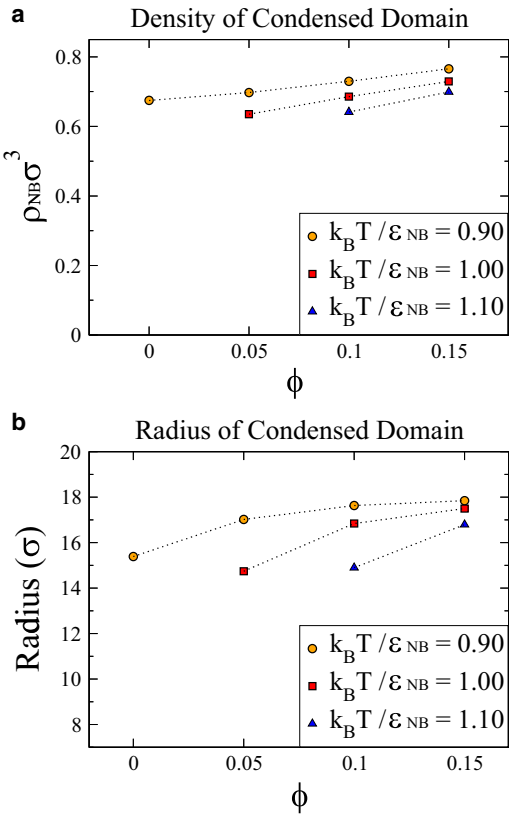

FIGURE 4 Density (*a*) and size (*b*) of a condensed domain. Data are presented only for cases in which the condensed domain forms.

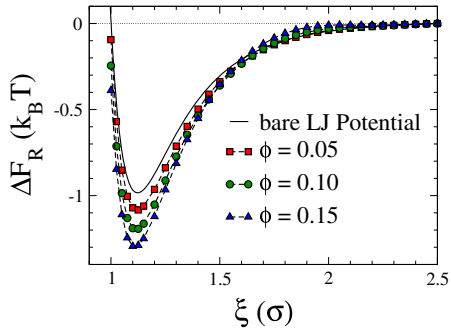

FIGURE 5 Effective potential between two NB particles as a function of distance ξ in units of σ. Those at crowding volume fractions of 0.05, 0.10, and 0.15 are compared with the bare LJ potential.

attraction well depth, ϵ_{NB}, by 0.1 k_BT corresponds to the change of k_BT/ϵ_{NB} by ~0.1. In Fig. 2 *a*, the phase separation occurs when k_BT/ϵ_{NB} is changed by 0.05 from 0.95 to 1.00, which implies that the change of k_BT/ϵ_{NB} by 0.1 due to crowding is large enough to dramatically change the phase behavior. Therefore, we conclude that the crowding-induced phase separation is a direct result of the increased intermolecular attractions. However, it is noted that the effective potential calculated in this way does not truly represent the effective potential between NB proteins and RNAs in vivo. The data in Fig. 5 were obtained between two free NB particles in a sea of crowders; however, many of the NB particles in Fig. 1 are not free and are surrounded by other NB particles in the condensed domain. Nevertheless, the effective potential in Fig. 5 directly provides a qualitative understanding of the induced phase separation in terms of the increased intermolecular interactions between NB particles due to crowding.

The increase of the effective attraction induced by crowding is explained in terms of the increase in the configurational entropy of crowders. When two reactants are separated far from each other, the crowders are excluded from the volume of $4\pi/3(r_{NB} + r_{crw})^3$ around each NB particle, where r_{NB} and r_{crw} are the radii of NB particles and crowders, respectively. When the two NB particles are in contact, the total excluded volume decreases, and thus more space is available for crowders and the configurational entropy of crowders increases. As a result, the close contact between the two NB particles is favored and increases the effective attraction in the crowded media (10,11,18,20,21,32). This entropic effect is called the depletion effect and has been investigated most actively in the study of colloid-polymer mixtures (21).

Physical consequences of crowding on diffusion and reaction

The crowding condition can be altered significantly by acute changes in cell volume that may occur due to changes in osmolarity under normal and pathological conditions (33).

In addition, it is also possible that the post-translational modification of some proteins can induce the assembly or disassembly of other NBs (3,22) and thus dramatically change the total amount of proteins in the nucleoplasm that can induce the crowding effect on a specific NB under investigation. For example, the hyperphosphorylation of coilin, the marker protein of Cajal bodies, results in the disassembly of the Cajal bodies (22), and it can be envisioned that the dispersed macromolecular components of the Cajal bodies can exert the crowding force on other NBs, such as PML NBs, with which the association of the Cajal body components is insignificant.

One of the major physical consequences of the change in the crowding condition is a change of the particle density in the condensed domain. The densities and volume fractions of the condensed and dilute phases under different crowding conditions are summarized in Table 1. By changing the crowder volume fraction from 0.05 to 0.15, the volume fraction of all of the particles, including NB particles and crowders within the condensed domain, changes from 0.333 to 0.383 and that of the dilute phase changes from 0.084 to 0.179. Such increases of volume fractions in and out of the condensed phase may have a huge impact on diffusive transport and macromolecular associations.

The transport of proteins and RNAs is a crucial step in every cellular process, and in particular those processed within NBs need to be exported out of the NBs, and in many cases even out to the cytoplasm, to play their biological roles. Therefore, we investigate the crowding effect on the transport of macromolecules by calculating the first passage time to certain distances within and out of a condensed domain. The first passage time is calculated for central NB particles, defined as those localized within a central spherical volume with a radius of 3.0σ from the center of mass of the condensed domain. From the simulation trajectories, the times required for the central NB particles to reach two critical distances, $r_c = 10\sigma$ and 20σ, are evaluated to give the average first passage times. The two critical distances are chosen because the average radius of the condensed domain ranges between 14.7σ and 17.8σ for $k_BT/\epsilon_{NB} = 0.90$ and 1.00, as shown in Fig. 4, and therefore the first passage times to $r_c = 10\sigma$ and 20σ correspond to the rate of transport within and out of the condensed phase, respectively.

As the crowding volume fraction increases, the first passage times within and out of the condensed domain increase because the diffusion of NB particles becomes more difficult due to the increased particle volume fractions ϕ_{dense} and ϕ_{dilute}, as summarized in Table 1. In Fig. 6, the first passage time within the condensed domain increases by 1.4 times from $\phi = 0.05$ to 0.15 at both $k_BT/\epsilon_{NB} = 0.90$ and 1.00. However, the first passage time out of the condensed domain increases by 2.3-fold from $\phi = 0.05$ to 0.15, and therefore the delay due to crowding is more pronounced when NB particles are exported out of the condensed domain. This implies that NB particles are likely to be retained longer close to the condensed domain under more crowded conditions.

It has been shown that several macromolecular associations occur within NBs. One example of such an association is the assembly of U4/U6 spliceosomal di-snRNPs. Although this process is also observed to occur in the nucleoplasm when cells lack Cajal bodies, Klingauf et al. (25) showed, using a mathematical modeling approach, that the formation of Cajal bodies can increase the assembly of U4/U6 di-snRNPs by 11-fold. On the basis of this result, the authors suggested that the rate of various macromolecular association can also be promoted in several other NBs. The increased association rate within Cajal bodies

TABLE 1 Total particle densities and volume fractions in condensed and dilute phases, for varying volume fractions of crowders ϕ, calculated at $k_BT/\epsilon_{NB} = 1.00$

ϕ	$\rho_{dense}\sigma^3$	$\rho_{dilute}\sigma^3$	ϕ_{dense}	ϕ_{dilute}
0.05	0.6365	0.1604	0.333	0.084
0.10	0.6870	0.2460	0.360	0.129
0.15	0.7309	0.3427	0.383	0.179

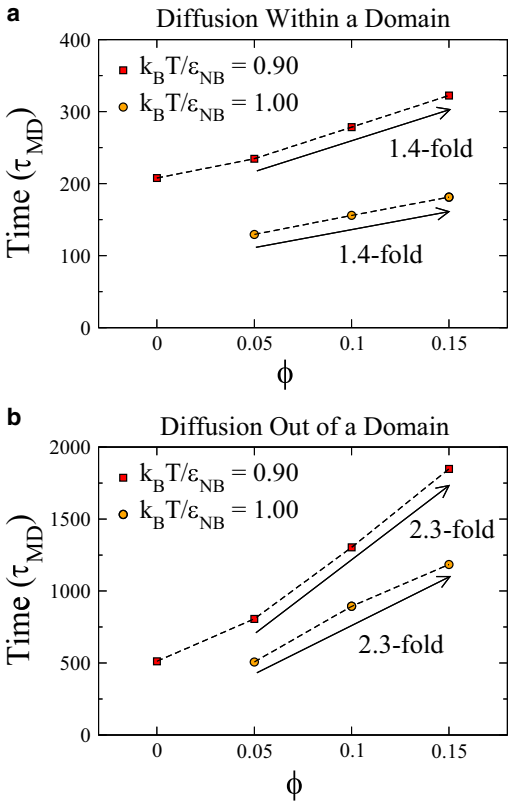

FIGURE 6 First passage time required for NB particles in the center of a condensed domain to reach a radial distance of 10σ and 20σ at different crowder volume fractions. First passage times are calculated at $k_BT/\epsilon_{NB} = 0.90$ and 1.00. Because the domain does not form at $\phi = 0.00$ and $k_BT/\epsilon_{NB} = 1.00$, a point is missing there.

was mostly ascribed to the 20-fold increase of the U4 snRNA concentration in the Cajal bodies compared with that in the nucleoplasm. However, in this modeling approach, the presence of a high content of macromolecules other than U4 and U6 RNPs is not considered. Because the macromolecular concentration in the NBs is affected significantly by crowding in the nucleoplasm, as shown in Table 1, we investigate the crowding effect on the macromolecular associations that occur within NBs when the crowding volume fraction is changed.

As detailed in the Supporting Material, we study the crowding effect on macromolecular associations using a theoretical expression of the rate constant from the modified Smoluchowski equation (31,34). This method has been verified previously in comparison with Brownian dynamics simulations (13,14). In this model, the reaction between two hard spherical reactants is determined on each collision by a parameter called the reaction probability, p_{rxn} (13,14). The overall reaction rate constant, k, can be written as

$$\frac{1}{k} = \frac{1}{k_D} + \frac{1}{k_{trs}}, \tag{2}$$

where k_D is the diffusion controlled reaction rate constant expressed as $4\pi\sigma D_{rel}$, and k_{trs} is the transition-state limited rate constant expressed as $p_{rxn}k_0g(\sigma)$. D_{rel} is the sum of diffusion coefficients D of two reactants, σ is the particle diameter or collision diameter, k_0 is the intrinsic rate constant, and $g(\sigma)$ is the radial distribution at contact.

It was previously shown that the reaction rate can be either accelerated or decelerated with crowding, depending on the reaction probability on collision p_{rxn} (13,14). Such contrasting results for the reaction rate were explained in terms of the competing contributions at different p_{rxn} -values from two opposing effects of crowding: the reduced diffusion rate of reactants and the increased probability of recollision between reactants caused by their increased local density near each other (13,14). In Eq. 2, the inverse of the reaction rate constant k is determined by a sum of the inverse of k_D and that of k_{trs}. It can be understood from the inverse relation that, between k_D and k_{trs}, the one with a smaller value contributes more significantly to the determination of k. When the reaction probability on collision is very small $(p_{rxn} < 0.01)$, the value of k_{trs} becomes much smaller than that of k_D, and thus k is determined mostly by k_{trs}. Because the local density $g(\sigma)$ increases with crowding, both k and k_{trs} increase as the crowder volume fraction increases and the macromolecular association is accelerated. On the other hand, when p_{rxn} is close to 1.00, the value of k_D is smaller than that of k_{trs}, and therefore k_D determines k. As the crowder volume fraction increases, the diffusion rate of reactants is reduced, resulting in the decrease in k as well as k_D, and the macromolecular association is decelerated. In this work, we choose the value of the reaction probability $p_{rxn} = 4.70 \times 10^{-7}$ to mimic the reactive patch spanned by a polar angle of 3°, as described in the Supporting Material.

The changes in the volume fraction of the condensed domain, ϕ_{dense}, at different crowder volume fractions, ϕ, are given in Table 2. The corresponding changes in the diffusion coefficient D/D_0, the local density or radial distribution at contact $g(\sigma)$, the diffusion controlled rate constant k_D, the transition-state limited rate constant k_{trs}, and the overall reaction rate constant k are also summarized in Table 2. Obviously, the diffusion rate of reactants becomes slower under more crowded conditions, and so does k_D, which depends on the diffusion rate. On the other hand, the local density $g(\sigma)$ increases with crowding, and k_{trs}, depending on $g(\sigma)$, also increases with crowding. It is noted that the change in k shown in Table 2 is very similar to that of k_{trs}. This is because the value of p_{rxn} is so small that k_{trs} contributes more to the determination of k.

The increase in density within NBs due to crowding in the nucleoplasm is likely to increase the chance of macromolecular associations. In our simulations, when the crowder volume fraction increases from 0.05 to 0.15, the volume fraction of the condensed domain changes from 0.333 to 0.383. The overall reaction rate constant k increases from 3.42×10^5 to 4.13×10^5, corresponding to the acceleration of association reactions by 21%. Although this 21% acceleration of macromolecular associations is small, it may have significant consequences for various cellular processes. If several association reactions occur in a cascade, the accelerating effect can become pronounced to several powers of 21% acceleration. In conclusion, the rate of macromolecular associations is accelerated by the density increase in the condensed domain, which is originally induced by the increased density of crowders.

As mentioned above, crowding conditions in cells may be altered significantly by acute changes in cell volume regulated by external stresses under normal and pathological conditions (33). In addition to the change in the crowding condition, the cell volume change has been associated with a variety of biological functions, such as regulation of metabolism, hormone release, cell proliferation, and cell death (33,35), in which one can envision a possible role for crowding. However, due to the divergent roles of crowding in the stability of macromolecular complexes and the dynamics of the constituting macromolecules, we limit our discussion to a few physical consequences that might affect various biological functions. Whether such

TABLE 2 Prediction of the rate constant k ($M^{-1}s^{-1}$) in the condensed domain (NBs), for varying volume fractions of crowders ϕ, calculated at $k_BT/\epsilon_{NB} = 1.00$

ϕ	ϕ_{dense}	D/D_0	$g(\sigma)$	k_D	k_{trs}	k
0.05	0.333	0.334	2.809	1.77×10^7	3.48×10^5	3.42×10^5
0.10	0.360	0.280	3.128	1.48×10^7	3.88×10^5	3.78×10^5
0.15	0.383	0.234	3.442	1.24×10^7	4.27×10^5	4.13×10^5

physical consequences are favorable depends on the location of their functions. If a certain biological process regulated by NB particles occurs within NBs, an increase in macromolecular crowding will certainly have a favorable effect, such as the acceleration of macromolecular associations. However, if other biological processes regulated by processed NB particles occur outside of the NBs, the increase in crowding is likely to delay the process by reducing the rate of transport out of the NBs. The reverse effect of crowding may be discussed in terms of the physical consequences when the crowder volume fraction is decreased. Therefore, we speculate that regulation of the crowding condition in a timely manner during the cell cycle (i.e., increasing or decreasing crowding) may facilitate coordinated biological processes.

To better understand the biological implications of the physical consequences induced by macromolecular crowding and its resulting alterations, we need to quantify the concentrations of macromolecules at specific locations and times in a live cell. Studies to that end are under way (36), and it is hoped that such efforts will deepen our understanding of crowding effects under normal and pathological conditions, in the course of cell cycles or in different stages of carcinogenesis.

CONCLUSIONS

The phase separation and thus the self-assembly of NB proteins and RNAs are significantly promoted in a crowded environment. The facilitated phase separation induced by the presence of volume-exclusive crowders helps explain the experimental observation of crowding-controlled NB formation. A direct interpretation is provided by the increase of the effective attraction calculated between NB particles when the crowder volume fraction increases.

The addition of crowders increases the particle volume fractions in both the condensed and dilute phases. Due to the increased particle volume fractions, the diffusive transport of macromolecules within and out of NBs is delayed. The delay is more significant in the case of macromolecules going out of the NBs, and therefore implies a longer residence in NBs. The density increase in the condensed domain also has an impact on the macromolecular associations that occur within NBs, resulting in accelerations of ~21%. The delayed transportation and accelerated macromolecular associations may significantly affect biological processes regulated by body-specific proteins and RNAs.

To capture the basic physical principles of the crowding effect, we used simple spherical particles whose phase separation has physical similarities to NB formation. In future work, we plan to develop more sophisticated models of NB proteins. For instance, it was shown that relatively large macromolecules can penetrate deeply into NBs rather easily (37), in contrast to our simulations, in which the density of non-NB particles (referring to crowders) is extremely low in the condensed domain. The introduction of nonspherical structure and anisotropic attraction between NB particles may allow the deep penetration of large macromolecules into the condensed domain by forming a less dense domain.

Although not many experimental data concerning the role of crowding in specific biological functions are available, one can expect that it is very important, because all biological processes occur in a crowded cellular environment. Continuing efforts to elucidate crowding effects should provide significant insights into biological processes in vivo, including the cellular organization of genomes and its impact on genome regulation. For such purposes, the quantitative characterization of macromolecular contents at specific locations and times in a live cell is the first requirement to move forward.

SUPPORTING MATERIAL

Methods and references (38–43) are available at http://www.biophysj.org/biophysj/supplemental/S0006-3495(12)00778-3.

This research was supported by the National Research Foundation of Korea under grants NRF-2011-0024621 and NRF-2011-220-C00030, and by an Ewha Global Top 5 Grant 2011 from Ewha Womans University.

REFERENCES

1. Misteli, T. 2007. Beyond the sequence: cellular organization of genome function. *Cell.* 128:787–800.
2. Matera, A. G., M. Izaguire-Sierra, …, T. K. Rajendra. 2009. Nuclear bodies: random aggregates of sticky proteins or crucibles of macromolecular assembly? *Dev. Cell.* 17:639–647.
3. Dundr, M., and T. Misteli. 2010. Biogenesis of nuclear bodies. *Cold Spring Harb. Perspect. Biol.* 2:a000711.
4. Brangwynne, C. P. 2011. Soft active aggregates: mechanics, dynamics and self-assembly of liquid-like intracellular protein bodies. *Soft Matter.* 7:3052–3059.
5. Mao, Y. S., B. Zhang, and D. L. Spector. 2011. Biogenesis and function of nuclear bodies. *Trends Genet.* 27:295–306.
6. Mao, Y. S., H. Sunwoo, …, D. L. Spector. 2011. Direct visualization of the co-transcriptional assembly of a nuclear body by noncoding RNAs. *Nat. Cell Biol.* 13:95–101.
7. Kaiser, T. E., R. V. Intine, and M. Dundr. 2008. De novo formation of a subnuclear body. *Science.* 322:1713–1717.
8. Shevtsov, S. P., and M. Dundr. 2011. Nucleation of nuclear bodies by RNA. *Nat. Cell Biol.* 13:167–173.
9. Bickmore, W. A., and H. G. E. Sutherland. 2002. Addressing protein localization within the nucleus. *EMBO J.* 21:1248–1254.
10. Minton, A. P. 1998. Molecular crowding: analysis of effects of high concentrations of inert cosolutes on biochemical equilibria and rates in terms of volume exclusion. *Methods Enzymol.* 295:127–149.
11. Zhou, H.-X., G. Rivas, and A. P. Minton. 2008. Macromolecular crowding and confinement: biochemical, biophysical, and potential physiological consequences. *Annu. Rev. Biophys.* 37:375–397.
12. Kozer, N., and G. Schreiber. 2004. Effect of crowding on protein-protein association rates: fundamental differences between low and high mass crowding agents. *J. Mol. Biol.* 336:763–774.
13. Kim, J. S., and A. Yethiraj. 2009. Effect of macromolecular crowding on reaction rates: a computational and theoretical study. *Biophys. J.* 96:1333–1340.

14. Kim, J. S., and A. Yethiraj. 2010. Crowding effects on association reactions at membranes. *Biophys. J.* 98:951–958.

15. Hancock, R. 2004. A role for macromolecular crowding effects in the assembly and function of compartments in the nucleus. *J. Struct. Biol.* 146:281–290.

16. Albiez, H., M. Cremer, …, T. Cremer. 2006. Chromatin domains and the interchromatin compartment form structurally defined and functionally interacting nuclear networks. *Chromosome Res.* 14:707–733.

17. Richter, K., M. Nessling, and P. Lichter. 2007. Experimental evidence for the influence of molecular crowding on nuclear architecture. *J. Cell Sci.* 120:1673–1680.

18. Marenduzzo, D., C. Micheletti, and P. R. Cook. 2006. Entropy-driven genome organization. *Biophys. J.* 90:3712–3721.

19. Kim, J. S., V. Backman, and I. Szleifer. 2011. Crowding-induced structural alterations of random-loop chromosome model. *Phys. Rev. Lett.* 106:168102.

20. Kim, J. S., and I. Szleifer. 2010. Depletion effect on polymers induced by small depleting spheres. *J. Phys. Chem. C.* 114:20864–20869.

21. Asakura, S., and F. Oosawa. 1958. Interaction between particles suspended in solutions of macromolecules. *J. Polym. Sci.* 33:183.

22. Hebert, M. D., and A. G. Matera. 2000. Self-association of coilin reveals a common theme in nuclear body localization. *Mol. Biol. Cell.* 11:4159–4171.

23. Shaw, D. E., P. Maragakis, …, W. Wriggers. 2010. Atomic-level characterization of the structural dynamics of proteins. *Science.* 330: 341–346.

24. Cho, E. J., and J. S. Kim. 2012. Crowding-induced phase separation of Lennard-Jones particles: implications to nuclear structures in a biological cell. *J. Phys. Chem. B.* 116:3874–3879.

25. Klingauf, M., D. Staněk, and K. M. Neugebauer. 2006. Enhancement of U4/U6 small nuclear ribonucleoprotein particle association in Cajal bodies predicted by mathematical modeling. *Mol. Biol. Cell.* 17:4972–4981.

26. Roy, S., and S. K. Das. 2012. Nucleation and growth of droplets in vapor-liquid transitions. *Phys. Rev. E.* 85:050602 (R).

27. Van Der Spoel, D., E. Lindahl, …, H. J. Berendsen. 2005. GROMACS: fast, flexible, and free. *J. Comput. Chem.* 26:1701–1718.

28. Handwerger, K. E., J. A. Cordero, and J. G. Gall. 2005. Cajal bodies, nucleoli, and speckles in the Xenopus oocyte nucleus have a low-density, sponge-like structure. *Mol. Biol. Cell.* 16:202–211.

29. Vrabec, J., G. K. Kedia, …, H. Hasse. 2006. Comprehensive study of the vapour-liquid coexistence of the truncated and shifted Lennard-Jones fluid including planar and spherical interface properties. *Mol. Phys.* 104:1509–1527.

30. Cheng, S., J. B. Lechman, …, G. S. Grest. 2011. Evaporation of Lennard-Jones fluids. *J. Chem. Phys.* 134:224704.

31. Zhou, H. X., and A. Szabo. 1991. Comparison between molecular dynamics simulations and the Smoluchowski theory of reactions in a hard-sphere liquid. *J. Chem. Phys.* 95:5948–5952.

32. Ellis, R. J., and A. P. Minton. 2003. Cell biology: join the crowd. *Nature.* 425:27–28.

33. Lang, F., G. L. Busch, …, D. Häussinger. 1998. Functional significance of cell volume regulatory mechanisms. *Physiol. Rev.* 78:247–306.

34. Szabo, A. 1989. Theory of diffusion-influenced fluorescence quenching. *J. Phys. Chem.* 93:6929–6939.

35. Hoffmann, E. K., I. H. Lambert, and S. F. Pedersen. 2009. Physiology of cell volume regulation in vertebrates. *Physiol. Rev.* 89:193–277.

36. Strasser, S. D., G. Shekhawat, …, V. Backman. 2012. Near-field penetrating optical microscopy: a live cell nanoscale refractive index measurement technique for quantification of internal macromolecular density. *Opt. Lett.* 37:506–508.

37. Verschure, P. J., I. van der Kraan, …, R. van Driel. 2003. Condensed chromatin domains in the mammalian nucleus are accessible to large macromolecules. *EMBO Rep.* 4:861–866.

38. Trzesniak, D., A.-P. E. Kunz, and W. F. van Gunsteren. 2007. A comparison of methods to compute the potential of mean force. *ChemPhysChem.* 8:162–169.

39. Hess, B., C. Holm, and N. van der Vegt. 2006. Osmotic coefficients of atomistic NaCl (aq) force fields. *J. Chem. Phys.* 124:164509.

40. Carnahan, N. F., and K. E. Starling. 1969. Equation of state for nonattracting rigid spheres. *J. Chem. Phys.* 51:635–636.

41. Hanna, S., W. Hess, and R. Klein. 1982. Self-diffusion of spherical Brownian particles with hard-core interaction. *Physica A.* 111: 181–199.

42. Barzykin, A. V., and A. I. Shushin. 2001. Effect of anisotropic reactivity on the rate of diffusion-controlled reactions: comparative analysis of the models of patches and hemispheres. *Biophys. J.* 80: 2062–2073.

43. Shoup, D., G. Lipari, and A. Szabo. 1981. Diffusion-controlled bimolecular reaction rates. The effect of rotational diffusion and orientation constraints. *Biophys. J.* 36:697–714.